Electrochemistry Communications 124 (2021) 106941

Contents lists available at ScienceDirect

Electrochemistry Communications

journal homepage: www.elsevier.com/locate/elecom

Short Communication

PEM electrolyzer characterization with carbon-based hardware and material sets

James L. Young [a], Zhenye Kang [a], Fabrizio Ganci [a,b], Steven Madachy [a], Guido Bender [a,*]

[a] National Renewable Energy Laboratory, Golden, CO, USA
[b] University of Palermo, Palermo, Italy

ARTICLE INFO

Keywords:
Water electrolysis
Carbon paper
Carbonorrosion
In situ characterization
Initial performance
PEMWE

ABSTRACT

The research and development of proton exchange membrane water electrolysis (PEMWE) is an upcoming and growing area due to a rising interest in hydrogen as an energy carrier. Operating conditions are harsher than in a fuel cell system, particularly because the potentials required for the oxygen evolution reaction are significantly higher. In commercial water electrolysis systems, this is compensated by typically using titanium material sets that are often protected against oxidation through coating processes. Such material choices make small scale research hardware and porous transport layers expensive and difficult to source. In this work, we show that the stability of traditional, carbon-based fuel cell materials such as porous transport layers and graphite flow fields can be sufficient for electrolyzer initial performance characterization procedures such as cell conditioning, a limited number of polarization curve measurements, and electrochemical impedance spectroscopy. We identify and quantify the onset of carbon degradation in porous transport layers with regards to operating length and define a strategy that enables the utilization of standard fuel cell hardware for short-term PEMWE experiments. With the knowledge that existing fuel cell material sets can be applied to conduct electrolyzer research when adhering to such limitations, fuel cell research hardware and experience can be more readily transferred to the younger and rapidly growing electrolysis research field.

1. Introduction

Fuel cell research and development efforts have a 20^{+}-year history which has resulted in considerable existing research and development capabilities at many institutions. More recently, awareness of the value of H_2 beyond its use in fuel cells is increasing. Emerging concepts also emphasize H_2 as commodity chemical in various industrial sectors and as an energy storage medium that supports electrical distribution networks [1–3]. While electrolytic hydrogen production offers a clean and efficient generation pathway, catalyst development and integration studies are still needed for the development of economically viable systems [4–7]. However, the link between *ex-situ* catalyst results and *in situ*performance is not as established for electrolysis electrocatalysts as it is for fuel cell electrocatalysts. Consequently, *in situ* evaluation of catalyst and/or electrode is currently a pathway that is required for advancing electrolysis systems. Fortunately, the complexity of the system needed to operate water electrolysis cells [8–10] is generally simpler than that required for fuel cells [11–13], which could allow for an easy transition from fuel cell research to electrolysis research even for small research groups.

Over the decades of fuel cell research, a specific fuel cell research hardware configuration has become widely accepted for material development work that requires typical performance and durability tests on subscale cells. This hardware consists of thick endplates often made of aluminum, gold plated copper current collectors that are insulated from the endplate with a sheet material, and graphite flow fields that typically contain a serpentine flow channel structure [14–16]. The diffusion media materials that are typically used in the cell are carbon-fiber based and wet-proofed with a hydrophobic polymer treatment.

Relative to fuel cells, proton exchange membrane water electrolysis (PEMWE) cells experience harsher conditions during operation. To enable the oxygen evolution reaction (OER) they require an operating potential that exceeds 1.4 V at 80 °C and can even be higher than 2 V to achieve high current densities [17–19]. These potential conditions are critical to the durability of the anode where oxidation occurs and protons are generated, leading to a locally acidic environment [20–26]. While IrO_2 OER catalysts are relatively durable under extended operation [27–29], such conditions are known to be detrimental to carbon-

* Corresponding author.
E-mail address: Guido.Bender@nrel.gov (G. Bender).

https://doi.org/10.1016/j.elecom.2021.106941
Received 9 December 2020; Received in revised form 7 January 2021; Accepted 18 January 2021
Available online 30 January 2021

based materials, i.e. the diffusion layers and flow fields, commonly used in fuel cells [30–36]. Considerable understanding of these materials and their limitations within fuel cell operating conditions exists [37–40]. Prior to adopting the use of standard fuel cell hardware and gas diffusion layer (GDL) materials for use in electrolyzer research cells, the performance, durability and limitations of these materials need to be understood before they can be used in any research efforts.

The stability limitations of carbon-based materials in an electrolyzer anode are certainly expected to prevent their application in commercial systems [41–43]. In this study, we show that the short-term stability of carbon paper based porous transport layers (PTL) and graphite flow fields is sufficient for use in PEMWE initial performance testing. Such initial performance measurements are central to catalyst development, integration studies, and membrane electrode assembly optimization [44–49].

2. Materials and methods

Measurements were performed using an in-house built electrolyzer test station that featured the minimalistic equipment approach described in previous work [8]. The DI water supply is preheated by separate proportional-integral-derivative (PID) temperature controllers (Watlow) which are connected to resistive heating tape that is wrapped around approximately 2.5 m long sections of 6.35 mm stainless steel line. Those lines serve as DI water supply lines for the anode and cathode. A third PID controller is connected to pad heaters that are glued to the endplates of a regular fuel cell hardware. The control thermocouple is inserted directly into the anode flow field plate. A backpressure control system is available to regulate the cell outlet pressure. This system is employed at our laboratory to compensate for the high elevation and typically used to regulate the operating pressure to sea level ambient pressure of 1 bar absolute. A power supply (HP 6031A) sources current while a multimeter (Keithley Model 2000) with National Institute of Standards and Technology-traceable calibration records the cell voltage. A computer with MultiScan (Grandalytics) software provides the electronics control and data recording, and a custom LabVIEW program is used for regulating and logging the cell back pressure.

Electrolyzer measurements were performed using a standard fuel cell hardware with 25 cm^2 active area and graphite single serpentine flow fields (Fuel Cell Technologies). The PTL used was 0.35-mm thick Toray carbon paper with 5% Teflon wet proofing (TGP-H-120, Fuel Cell Earth). For context, the interfacial resistance of the carbon-based PTL (5 mOhm cm^2) is lower than that of Ti-based PTLs (20–35 mOhm cm^2) and higher than that of Ir-coated Ti PTL (2 mOhm cm^2) according to previous *in situ* measurements [9]. The cell was sealed with 0.25-mm thick PTFE gasket. A catalyst-coated membrane (CCM) based on Nafion 117 was fabricated by ultrasonic spraying (SonoTek) of catalyst inks containing commercial Ir oxide from Alfa Aesar (Premion Iridium (IV) oxide 99.99%) and Pt/C (50 wt.% Pt on Ketjenblack) for the anode and cathode sides, respectively, as well as D2020 Nafion ionomer solution (Ion Power). The detailed fabrication procedure can be found in previous publications [50]. The resulting catalyst loadings were 1.22 mg Ir/cm^2 and 0.033 mg Pt/cm^2 as measured by X-ray fluorescence (XRF) spectroscopy. We note that previous work with IrO_2 OER catalyst at similar loadings demonstrated stable performance for several hundred to thousands of hours [27–29]. Thus, the contribution of IrO_2 dissolution to the performance degradation observed in this work is assumed to be negligible, which enables interpretation of the results with regards to the stability and degradation of the carbon-based PTLs and flow fields. Microscopy images were conducted of PTL as well as flow field materials prior to and after cell operation using a Keyence VHX5000 digital microscope.

Before performing polarization curve (VI) measurements, the cell temperature was first increased and allowed to stabilize at 80°C with 50 ml/min DI water (nominally 18.2 MΩflowing through both the anode and cathode. The outlet pressure of both cell compartments was regulated to 1 bar absolute. A three-step conditioning sequence was conducted by sourcing 0.2 A/cm^2 for 30 min, 1 A/cm^2 for 30 min, and finally holding the cell at 1.7 V for 10 h. Subsequently, a series of 27 current-controlled VI measurements was performed. Each measurement included both an increasing and a decreasing current scan which were averaged to generate the VI curves presented in this work. Current density steps were 0.1 A/cm^2 up to 0.2 A/cm^2 and 0.2 A/cm^2 between 0.2 A/cm^2 and 3.0 A/cm^2. The voltage was capped to never exceed 3 V. Each constant-current step segment was held for 5 min, and the last 1 min of data was averaged for each segment. It took a total of 160 min to complete each VI measurement. Although often valuable, we did not perform EIS measurements during this testing sequence to avoid open-circuit cell conditions during the manual switching process that was required by the available equipment. Instead, we preferred to conduct an uninterrupted sequence of polarization curves. Note that open-circuit conditions between measurements tend to be transient and uncontrolled, and cycling from high voltage to open circuit conditions accelerates Ir dissolution[51,52]. These conditions however interesting, are not the focus of this work, which addresses the feasibility readily accessible, carbon-based PTL materials and graphite flow fields for initial electrode/catalyst integration studies.

3. Results and discussions

Fig. 1 shows initial performance results of the electrolyzer cell operated with carbon-fiber PTL and graphite flow fields. Fig. 1A shows the current and voltage vs. time during cell conditioning and Fig. 1B shows results from a subsequent series of 27 VI measurements. Throughout the first two 30-min steps of the conditioning sequence at 0.2 A/cm^2 and 1.0 A/cm^2, the cell performance improves as the voltage decreases. The cell performance continues to gradually improve during the following 10-h long 1.7-V hold, with the current density increasing by 0.043 A/cm^2 over the first five hours and by 0.012 A/cm^2 over the last five hours. The performance improvement with ongoing operation significantly slowed down at the end of the 10 h period. In the last hour it was 0.002 A/cm^2 (0.5%) and the cell conditioning was considered to be completed [8]. The data indicate that a conditioning process is taking place within the cell. This may be due to improved access to reaction sites or due to the development of favored transport pathways. In any case, no indications are apparent in the data that indicate any detrimental effects of carbon related degradation or deterioration.

Fig. 1B shows the results of the subsequent VI measurement sequence. Three subsets of VIs are discernable in the results, i.e. VIs #1–17, #18–20, and #21–27. The performances of VIs #1–17 are closely clustered together. Their results are essentially identical, and no effects of any degradation processes are apparent. Quantitatively, VIs #1–17 have a standard deviation of 4.4 mV and 6.7 mV at 1.0 A/cm^2 and 2.0 A/cm^2, respectively, which fall within the aforementioned 0.5% voltage stabilization threshold for completion of cell conditioning and compared to previously reported benchmarking data indicate excellent reproducibility rather than degradation [8]. The performance of the VI #18–20 subset diverges from that of the VI #1–17 subset at current densities above 1.5 A/cm^2. While the performance is stable within the VI #18–20 subset, the VI #20 operating voltage is higher than VI #17 by 14.7 mV and 18.2 mV at 1.0 A/cm^2 and 2.0 V/cm^2, respectively. An additional performance decline is apparent between the VI #18–20 subset and VI #21–27 subset. For example, at 2.0 A/cm^2 the performance of VI #21 is another 74.0 mV lower than VI #20 and a total of 92.2 mV lower than VI #17. In addition, each of the following VIs #21–27 show a performance decline with respect to the previous VI. In Fig. 1C, these trends are plotted against the VI measurement number for current densities of 1.0, 2.0, and 3.0 A/cm^2. The data suggest that a small amount of cell stabilization is occurring within VI #1–4 (Fig. 1C region i. shaded blue), which is indicated by a small voltage increase at 1.0 and 2.0 A/cm^2 and a decrease at 3.0 A/cm^2. Subsequent to VIs #1–4, the performance of the cell is stable over an additional eight VI measurements (Fig. 1C region ii. shaded green). The results of VI #13,

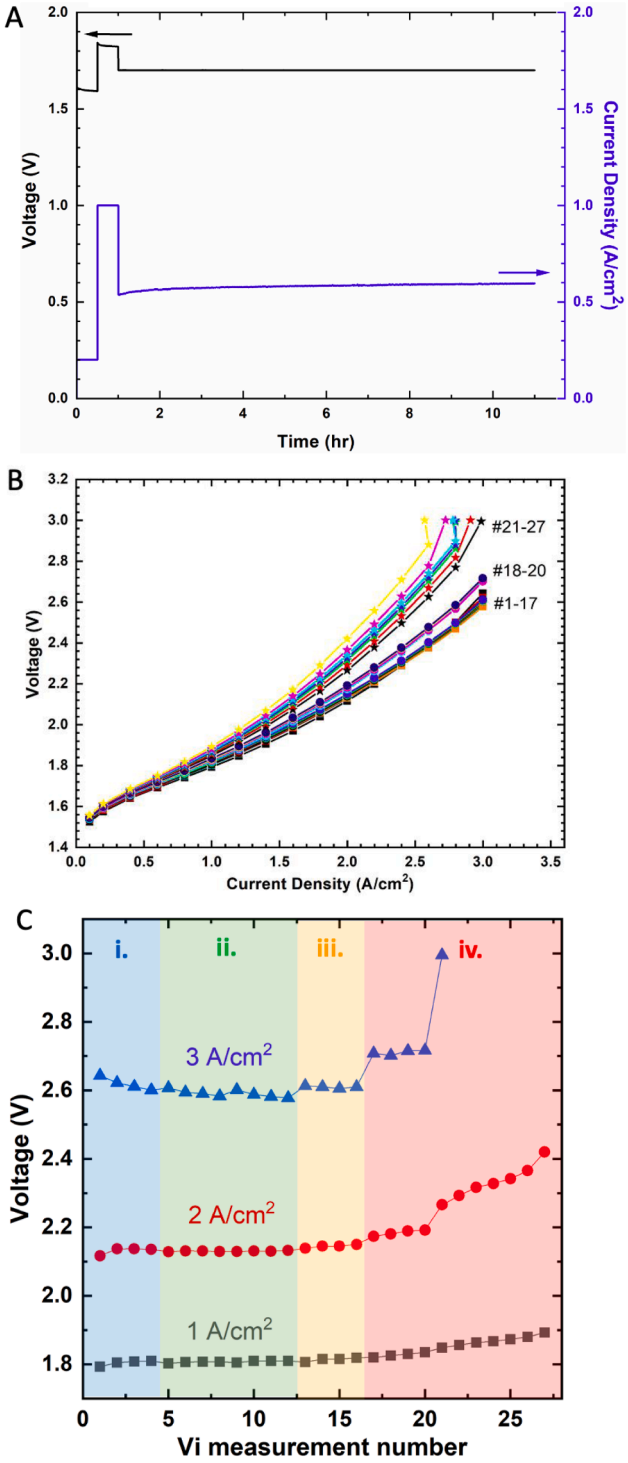

Fig. 1. Measurement sequence of electrolyzer cell using carbon PTLs and graphite flow fields. a) Cell conditioning sequence of 0.2 A/cm^2 for 30 min, 1 A/cm^2 for 30 min, and 1.7 V for 10 h b) subsequent VI measurement series, c) voltage stability for the same VI measurement series plotted for current densities of 1, 2, and 3 A/cm^2.

indicate the first signs of a performance decline that may be related to cell degradation. This decline proceeds in subsequent measurements (Fig. 1C region iii. shaded yellow), being more pronounced at a high current density of 3.0 A/cm^2. At VI #17 and after (Fig. 1C region iv. shaded red), the voltage at 3.0 A/cm^2 jumps and the voltage at 1.0 A/cm^2 and 2.0 A/cm^2 increases steadily with each measurement. After VI #21, the cell limit of 3 V was reached at 3.0 A/cm^2 for the first time. Note that the initial VI stability, which is likely dominated by the degradation of the carbon PTL material, is expected to improve when the voltage range is limited to values significantly below 3 V, such as for example 2.5 V or 2 V.

Fig. 2 shows imaging results from both the anode carbon paper PTL and the anode graphite flow field subsequent to conducting the experimental matrix. Fig. 2A shows the top view of the electrode-facing side of the anode PTL, with the inset showing the same section at a lower resolution. Within the marked circles of the images, the anode PTL contains a hole that likely originated from degradation processes that occurred during operation. The Fig. 2A inset also shows a dark line at the location of the hole. Such lines appeared at the locations where the edge of the anode flow field "land" areas make contact to the PTL. The discoloration seems to be related to increased anode PTL degradation along the interface from land to channel, which is also a location of increased physical stress. At the perimeter of the flow field land areas the PTL materials undergo an abrupt transition from a high compression under the land to a low compression within the flow channel. This causes mechanical deflection and may weaken the PTL fibers. In addition, the current density distribution also transitions at the land/edge from

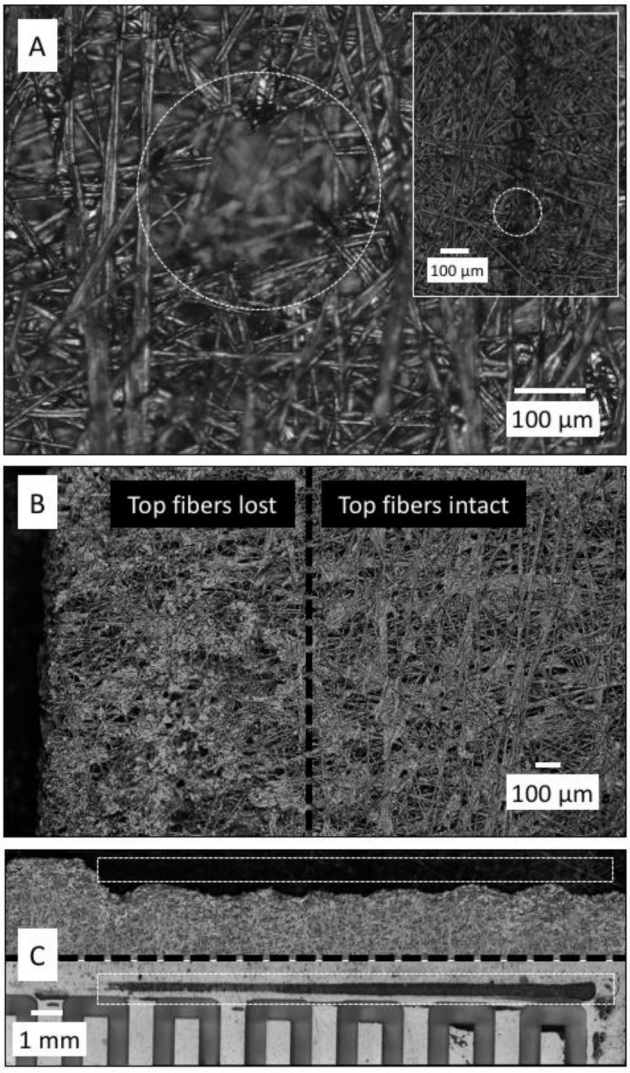

Fig. 2. Limits of carbon PTL on cell anode side. A) Initial failure/corrosion of PTL carbon fibers, B) loss of top PTL fibers at PTL perimeter, and C) extreme example of unchecked durability testing that will lead to severe corrosion of carbon PTL perimeter and direct contact between the MEA and graphite flow field, which can cause graphite pitting damage.

primarily through-plane over the land area to primarily in-plane over the channel area. The darker discolored lines shown in the Fig. 2A inset correspond with this transition area. The discoloration could be the result of loss of PTFE coating on the carbon fibers and subsequent texturing caused by carbon fiber corrosion. As Fig. 2A shows, this mechanism can progress into a pinhole which reduces electrical contact and will eventually lead to loss of performance. The degradation process may thus increase ohmic losses followed by decreasing catalyst utilization especially for electrode layers with low lateral conductivity like the unsupported, low-loading Ir anode catalyst layers used in this work.

Fig. 2B shows another prevalent area of PTL degradation which was observed within about 1 mm of the perimeter of the anode carbon paper PTL. In this edge area, a loss of the topmost layer of carbon fibers is apparent at the surface facing the anode electrode (Fig. 2B left side). If this corrosion process at the perimeter of the PTL is left unchecked for an excessive amount of time, disintegration of PTL material will occur at the edge. Fig. 2C shows an extreme example of the undesired consequences of extended operation which resulted in the loss of anode PTL integrity and geometry at the perimeter. In this extreme case, the extended operation resulted in direct contact between the CCM and the graphite flow field which caused pitting and destruction of the graphite flow field. The impacted areas are indicated by the white rectangle and shown as top view images of the PTL (top) which is missing the edge, and the flow field (bottom) which is significantly pitted. It is likely that the acidic nature of the membrane and/or ionomer in an oxidative environment, i.e., potentials of >1.2 V vs. reversible hydrogen electrode where the carbon oxidation rate becomes appreciable [53], has contributed to the corrosion of the anode graphite flow field. For this reason, direct contact of the MEA to the graphite flow field must be avoided to prevent flow field damage.

4. Conclusions

This work investigates the utilization of commonly available carbon-based fuel cell materials and hardware for PEM water electrolysis research. The results imply that Ti-based material sets are not ultimately required for all PEMWE research needs. Instead, cheaper and more readily available graphite materials may be used in specific cases. The presented results indicate that carbon-based material sets are sufficient for characterizing initial electrolyzer performance, however, they have limitations for extended utilization at the anode electrode. The longevity of the representative carbon materials tested was adequate for performing a 10 h cell conditioning procedure followed by twelve, 2.5-h long polarization curve measurements before any performance losses were observed. This result translates into 40 h of allowable operation that included 15 h of operation between 2 V and 3 V.

Based on this work, PEMWE research that requires material screening in MEA components, such as material development R&D, can safely utilize traditional fuel cell hardware and materials within the demonstrated set of conditions. Operation outside of these conditions leads to performance degradation of the cell due to carbon corrosion predominantly along the land/channel transition area and the perimeter of the anode PTL. Excessive periods of operation may further result in pitting and destruction of the anode flow field and are highly unadvised. Furthermore, contact between membrane and graphite must be avoided, which might occur by MEA misalignment during assembly or over-use of carbon PTL without replacement.

In summary, existing fuel cell materials and hardware can be applied to electrolyzer research adhering to the associated limitations. Thus, fuel cell research assets can be more readily transferred to the younger and rapidly growing electrolysis research field.

CRediT authorship contribution statement

James L. Young: Conceptualization, Investigation, Writing - original draft. **Zhenye Kang:** Conceptualization, Writing - review & editing. **Fabrizio Ganci:** Investigation, Writing - review & editing. **Steven Madachy:** Investigation, Writing - review & editing. **Guido Bender:** Conceptualization, Writing - review & editing, Supervision.

Declaration of Competing Interest

The authors declare that they have no known competing financial interests or personal relationships that could have appeared to influence the work reported in this paper.

Acknowledgements

This work was authored by the National Renewable Energy Laboratory, operated by Alliance for Sustainable Energy, LLC, for the U.S. Department of Energy (DOE) under Contract No. DE-AC36-08GO28308. Funding was provided by the U.S. Department of Energy Office of Energy Efficiency and Renewable Energy (EERE) Hydrogen and Fuel Cell Technologies Office (HFTO). The views expressed in the article do not necessarily represent the views of the DOE or the U.S. Government. The U.S. Government retains and the publisher, by accepting the article for publication, acknowledges that the U.S. Government retains a nonexclusive, paid-up, irrevocable, worldwide license to publish or reproduce the published form of this work, or allow others to do so, for U.S. Government purposes. The authors would like to acknowledge Dr. Marcelo Carmo from the Forschungszentrum Jülich for fruitful discussions and the provision of MEA samples. The authors would further like to acknowledge Trent Guerrero for assistance with literature search and review and Dr. Shaun Alia from the National Renewable Energy Laboratory for valuable discussions.

References

[1] B. Pivovar, N. Rustagi, S. Satyapal, The Electrochemical Society Interface 27 (2018) 47–52.
[2] Y. Zhang, C. Wang, N. Wan, Z. Liu, Z. Mao, Electrochemistry Communications 9 (2007) 667–670.
[3] M. Carmo, D.L. Fritz, J. Mergel, D. Stolten, International Journal of Hydrogen Energy 38 (2013) 4901–4934.
[4] Z. Kang, J. Mo, G. Yang, S.T. Retterer, D.A. Cullen, T.J. Toops, J.B. Green Jr, M. M. Mench, F.-Y. Zhang, Energy & Environmental Science 10 (2017) 166–175.
[5] G. Song, Z. Wang, J. Sun, J. Sun, D. Yuan, L. Zhang, Electrochemistry Communications 105 (2019), 106487.
[6] Z. Wang, L. Zhang, Electrochemistry Communications 88 (2018) 29–33.
[7] Z. Kang, S.M. Alia, J.L. Young, G. Bender, Electrochimica Acta 354 (2020), 136641.
[8] G. Bender, M. Carmo, T. Smolinka, A. Gago, N. Danilovic, M. Mueller, F. Ganci, A. Fallisch, P. Lettenmeier, K. Friedrich, K. Ayers, P. Bryan, J. Mergel, D. Stolten, International Journal of Hydrogen Energy 44 (2019) 9174–9187.
[9] Z. Kang, S.M. Alia, M. Carmo, G. Bender, Journal of Power Sources 481 (2021), 229012.
[10] N. Briguglio, F. Panto, S. Siracusano, A. Arico, Electrochimica Acta (2020), 136153.
[11] M. Straumann, M. Dupont, D. Buttin, J.-C. Dubois, Fuel Cells Bulletin 3 (2000) 11–13.
[12] Ö.F. Selamet, F. Becerikli, M.D. Mat, Y. Kaplan, International Journal of Hydrogen Energy 36 (2011) 11480–11487.
[13] Fuel Cells Bulletin (2004).
[14] E. Engebretsen, G. Hinds, Q. Meyer, T. Mason, E. Brightman, L. Castanheira, P. R. Shearing, D.J. Brett, Journal of Power Sources 382 (2018) 38–44.
[15] L. Martins, J. Gardolinski, J. Vargas, J. Ordonez, S. Amico, M. Forte, Applied Thermal Engineering 29 (2009) 3036–3048.
[16] G. Hinds, Fuel Cells Bulletin 2013 (2013) 12–15.
[17] S. Zhao, A. Stocks, B. Rasimick, K. More, H. Xu, Journal of the Electrochemical Society 165 (2018) F82.
[18] R. Muntean, D.T. Pascal, U. Rost, L. Holtkotte, J. Näther, F. Köster, M. Underberg, T. Hülser, M. Brodmann, Topics in Catalysis 62 (2019) 429–438.
[19] T. Schuler, T. Kimura, T.J. Schmidt, F.N. Büchi, Energy & Environmental Science (2020).
[20] M. Langemann, D.L. Fritz, M. Müller, D. Stolten, International Journal of Hydrogen Energy 40 (2015) 11385–11391.
[21] P. Millet, R. Ngameni, S. Grigoriev, N. Mbemba, F. Brisset, A. Ranjbari, C. Etiévant, International Journal of Hydrogen Energy 35 (2010) 5043–5052.
[22] C. Mittelsteadt, T. Norman, M. Rich, J. Willey, PEM Electrolyzers and PEM regenerative fuel cells industrial view, in: Electrochemical Energy Storage for Renewable Sources and Grid Balancing, Elsevier, 2015, pp. 159–181.
[23] Z. Kang, G. Yang, J. Mo, Y. Li, S. Yu, D.A. Cullen, S.T. Retterer, T.J. Toops, G. Bender, B.S. Pivovar, F. Zhang, Nano Energy 47 (2018) 434–441.

[24] S. Ohyagi, T. Matsuda, Y. Iseki, T. Sasaki, C. Kaito, Journal of Power Sources 196 (2011) 3743–3749.
[25] Y. Wang, D.Y. Leung, J. Xuan, H. Wang, Renewable Sustainable Energy Reviews 65 (2016) 961–977.
[26] F. Khatib, T. Wilberforce, O. Ijaodola, E. Ogungbemi, Z. El-Hassan, A. Durrant, J. Thompson, A. Olabi, Renewable Sustainable Energy Reviews 111 (2019) 1–14.
[27] C. Capuano, K. Ayers, J. Manco, L. Wiles, S. Errico, I.V. Zenyuk, A.Z. Weber, A. Kusoglu, N. Danilovic, M. Ulsh, High efficiency PEM water electrolysis enabled by advanced catalysts, membranes and processes, in: ECS Meeting Abstracts, IOP Publishing, 2020, p. 2447.
[28] S.M. Alia, S. Stariha, R.L. Borup, Journal of the Electrochemical Society 166 (2019) F1164.
[29] H.X. PI, (2015).
[30] A. Hermann, T. Chaudhuri, P. Spagnol, International Journal of Hydrogen Energy 30 (2005) 1297–1302.
[31] A.L. Dicks, D.A. Rand, Fuel Cell Systems Explained, John Wiley & Sons, 2018.
[32] A.L. Dicks, Journal of Power Sources 156 (2006) 128–141.
[33] D.L. Maricle, D.C. Nagle, Carbon foam fuel cell components, in: Google Patents, 1978.
[34] M.M. Mench, Fuel Cell Engines, John Wiley & Sons, 2008.
[35] M. Wang, S. Medina, J.R. Pfeilsticker, S. Pylypenko, M. Ulsh, S.A. Mauger, ACS Applied Energy Materials 2 (2019) 7757–7761.
[36] M. Wang, G. Rome, S. Medina, J.R. Pfeilsticker, Z. Kang, S. Pylypenko, M. Ulsh, G. Bender, Journal of Power Sources 466 (2020), 228344.
[37] R. Borup, J. Meyers, B. Pivovar, Y.S. Kim, R. Mukundan, N. Garland, D. Myers, M. Wilson, F. Garzon, D. Wood, Chemical Reviews 107 (2007) 3904–3951.
[38] D.V. de BFA, G. Janssen, Fuel Cells, 8 (2008) 3–22.
[39] J. Wu, X.Z. Yuan, J.J. Martin, H. Wang, J. Zhang, J. Shen, S. Wu, W. Merida, Journal of Power Sources 184 (2008) 104–119.
[40] X. Wang, W. Li, Z. Chen, M. Waje, Y. Yan, Journal of Power Sources 158 (2006) 154–159.
[41] F. Yi, S. Chen, Journal of Hazardous Materials 157 (2008) 79–87.
[42] S. Siracusano, S. Trocino, N. Briguglio, F. Panto, A.S. Arico, Journal of Power Sources 468 (2020), 228390.
[43] F. Panto, S. Siracusano, N. Briguglio, A.S. Arico, Applied Energy 279 (2020), 115809.
[44] F. Fouda-Onana, M. Chandesris, V. Médeau, S. Chelghoum, D. Thoby, N. Guillet, International Journal of Hydrogen Energy 41 (2016) 16627–16636.
[45] C. Klose, P. Trinke, T. Böhm, B. Bensmann, S. Vierrath, R. Hanke-Rauschenbach, S. Thiele, Journal of the Electrochemical Society 165 (2018) F1271.
[46] P. Millet, N. Mbemba, S. Grigoriev, V. Fateev, A. Aukauloo, C. Etiévant, International Journal of Hydrogen Energy 36 (2011) 4134–4142.
[47] W. Xu, K. Scott, International Journal of Hydrogen Energy 35 (2010) 12029–12037.
[48] M.K. Debe, S. Hendricks, G. Vernstrom, M. Meyers, M. Brostrom, M. Stephens, Q. Chan, J. Willey, M. Hamden, C. Mittelsteadt, Journal of the Electrochemical Society 159 (2012) K165.
[49] S. Grigoriev, P. Millet, S. Volobuev, V. Fateev, International Journal of Hydrogen Energy 34 (2009) 4968–4973.
[50] J. Lopata, Z. Kang, J. Young, G. Bender, J. Weidner, S. Shimpalee, Journal of The Electrochemical Society 167 (2020), 064507.
[51] A. Weiß, A. Siebel, M. Bernt, T.-H. Shen, V. Tileli, H. Gasteiger, Journal of The Electrochemical Society 166 (2019) F487.
[52] S. Alia, H2@ Scale: Experimental Characterization of Durability of Advanced Electrolyzer Concepts in Dynamic Loading, in, 2018.
[53] Y. Yi, G. Weinberg, M. Prenzel, M. Greiner, S. Heumann, S. Becker, R. Schlögl, Catalysis Today 295 (2017) 32–40.